

MOL #42689

**TITLE**

**IN VIVO IMAGING REVEALS SELECTIVE PEROXISOME PROLIFERATOR  
ACTIVATED RECEPTOR MODULATOR (SPPARM) ACTIVITY OF THE SYNTHETIC  
LIGAND MK-886.**

Andrea Biserni, Fabio Giannessi, Anna Floriana Sciarroni, Ferdinando Maria Milazzo, Adriana  
Maggi and Paolo Ciana.

Center of Excellence on Neurodegenerative Diseases, Department of Pharmacological Sciences,  
University of Milan (A.B., P.C., A.M.), Via Balzaretti 9, 20133 Milan, Italy. TOP (Transgenic  
Operative Products) s.r.l. (A.B.), Via Einstein, Località Cascina Codazza, 26900 Lodi. Sigma-Tau  
Industrie Farmaceutiche Riunite S.p.A. (Department of Endocrinology and Metabolism) Pomezia  
(F.G., A.F.S., F.M.M.), Rome, Italy.

MOL #42689

**RUNNING TITLE**

**IN VIVO IMAGING REVEALS MK-886 SPPARM ACTIVITY IN MOUSE TESTIS.**

Corresponding Author: Adriana Maggi, Center of Excellence on Neurodegenerative Diseases,  
Department of Pharmacological Sciences, University of Milan, Via Balzaretti 9, 20133 Milan, Italy.

Phone: +39 02 50318375; Fax: +39 02 50318290 or +39 02 50318284; e-mail:  
adriana.maggi@unimi.it

Number of text pages: 30

Number of tables: 0

Number of figures: 7

Number of references: 47

Number of words in the Abstract: 126

Number of words in the Introduction: 631

Number of words in the Discussion: 1098

Non standard abbreviations:

NR = Nuclear Receptors; PPARs = Peroxisome Proliferator-Activated Receptors; RXRs = Retinoid-X-Receptors; PPRE = Peroxisome Proliferator Responsive Element; ERE = Estrogen Responsive Element; SPPARMs = Selective Peroxisome Proliferator-Activated Receptors Modulators; CMC = carbosimethylcellulose; CCD-camera = Charge-Coupled Device-camera; PRAT = Peri Renal Adipose Tissue.

MOL #42689

## ABSTRACT

We here report the finding of a new pharmacological activity of a well known antagonist of Peroxisome Proliferator-Activated Receptors (PPARs). PPARs belong to the family of nuclear receptors (NRs) playing a relevant role in mammalian physiology and are currently believed to represent a major target for the development of innovative drugs for metabolic and inflammatory diseases. In the present study, the application of reporter animal technology was instrumental to obtain the global pharmacological profiling indispensable to unravel MK-886 Selective Peroxisome Proliferator Activated Receptor Modulator (SPPARM) activity not underlined by previous traditional, cell-based studies. The results of the study, demonstrating the usefulness of reporter mice, may open new avenues for the development of innovative drugs for cardiovascular, endocrine, neural and skeletal systems characterized by limited side effects.

MOL #42689

Peroxisome proliferator-activated receptors (PPARs) are nuclear receptors (NRs) closely related to the thyroid hormone and retinoid receptors. The PPAR subfamily of nuclear receptors consists of three different receptors subtypes (PPAR $\alpha$ , PPAR $\beta/\delta$  and PPAR $\gamma$ ). Each member of the family, heterodimerizes with the Retinoid-X-Receptors (RXRs) and binds the responsive elements (PPREs, Peroxisome Proliferator Responsive Elements) in the promoter region of target genes (Kliwer et al., 1992; Tugwood et al., 1992) where, through interaction with other regulatory proteins, modulates their transcription. PPARs have been object of large attention as pharmacological targets because were shown to be involved in key physiological functions (lipid and glucose homeostasis, inflammatory processes and adipogenesis) (Anghel, 2007; Fruchart et al., 1999; Rosen et al., 2000; Kostadinova et al., 2005) and their malfunctioning has been associated with major disorders (metabolic syndrome, cardiovascular disease and diabetes) (Lehmann et al., 1995; Berger and Moller, 2002; Evans et al., 2004; Kota et al., 2005). Moreover, these receptors represent a novel potential pharmacological targets for the treatment of rare genetic diseases such as X-linked adrenoleukodistrophy (Albet et al., 1997; Rampler et al., 2003; Pujol et al., 2004). Thus PPARs may represent a new, most relevant target for drug development and have the potential to lead to the generation of treatments in areas where there is a major need for novel, efficacious drugs. Because of that, several pharmaceutical companies engaged their research in the identification of selective ligands for each PPAR subtype such as the PPAR $\gamma$  agonists thiazolidinediones developed for the treatment of diabetes, or dislipidemias. Yet, the pharmacological application of the PPAR ligands so far synthesized has been seriously hampered by their major side effects: such as liver toxicity (Watkins and Whitcomb, 1998; Gale, 2001; Graham et al., 2003; Masubuchi, 2006), negative effects on bone architecture and strength (Rzonca et al., 2004; Lazarenko et al., 2007), tumorigenesis (Berger et al., 2005; Shi et al., 2005) and cardiovascular events (Home et al., 2007; Nissen and Wolski, 2007; Psaty and Furberg, 2007). The difficulties for the development of novel drugs targeting PPARs replicate prior history with other members of the NRs family. Indeed the use of anti-inflammatory drugs targeting glucocorticoid receptors or estrogen receptors in hormonal

MOL #42689

replacement therapies for post-menopausal women has been limited by the severity of the side effects (Reeves et al., 2006; Conner, 2007; Woolf, 2007). Unquestionably, the ubiquitous expression, hallmark of some of the members of the NRs superfamily, represents a major obstacle to overcome for the development of drugs targeting PPARs, Estrogen Receptors and Glucocorticoid Receptors devoid of side effects. On the other hand, the progress in understanding the functions of co-regulators and their value in dictating NR tissue specificity of action (McKenna et al., 1999; Robyr et al., 2000; O'Malley, 2007), points to the practicability of projects aiming at finding ligands triggering a tissue-specific activation of NRs to be used in therapy. We believe that more appropriate model systems enabling a global view of drug activity in living organism would tremendously facilitate the identification of safer therapeutic molecules. On this line of thoughts, we recently generated a reporter mouse (namely the ERE-*Luc* mouse model) for the global screening of estrogen receptor ligands (Ciana et al., 2001; Maggi et al., 2004) and the strategy devised for this first model was further applied to create a reporter mouse for PPARs (PPRE-*Luc* mouse) (Ciana et al., 2007). The present study was undertaken to verify the suitability of the PPRE-*Luc* mouse for the pharmacological profiling of novel PPAR ligands. By identifying a new SPPARM activity of the well known PPAR $\alpha$  antagonist, MK-886, we here provide evidence of the powerfulness of the PPRE-*Luc* mouse model for the identification and characterization of PPAR ligands and show the superiority of this methodology, over the classical cell based tests, in the prediction of ligand potency and efficacy *in vivo*.

MOL #42689

## MATERIALS AND METHODS

### PPAR ligands

PPAR $\alpha$  ligands: Wy-14,643 (ChemSyn laboratories, Kansas City, KS, USA), MK-886 (Biomol International, Plymouth Meeting, PA, US), ST1929 (Sigma-Tau, Pomezia, Italy); PPAR $\beta/\sigma$  ligand: GW501516 (Axxora life sciences inc., San Diego, CA, USA); PPAR $\gamma$  ligands: Rosiglitazone (Axxora life sciences inc.), GW1929 (Sigma-Aldrich, St Louis, MO, US), GW9662 (Axxora life sciences inc.); dual PPAR $\alpha$  and  $\gamma$  ligands: ST2518 (Sigma-Tau).

### Experimental animals and pharmacological manipulations

Experiments performed in this study were conducted according to the “Guidelines for Care and Use of Experimental Animals”. Use of experimental animal was approved by the Italian Ministry of Research and University, and controlled by the panel of experts of the Department of Pharmacological Sciences, University of Milan. All experiments were carried on with male PPRE-*Luc* transgenic mice of 3-5 m of age. Mice were kept under a 12 h light–dark regimen. In order to maximize the reporter response to drug treatments, metabolic activation of PPARs was minimized by feeding mice only during the night (Ciana et al., 2007) for the 48 h preceding the experiment. All the experiments were carried out in the afternoon.

PPARs agonists and antagonists were administered s.c. (vehicle used: vegetal oil) or by gavage (vehicle used: water solution of 0,5% carbosimetilcellulose, CMC). All ligands were administered 50 and 250 mg/Kg s.c. or 50 mg/Kg by gavage with the following exceptions: rosiglitazone 10 and 50 mg/Kg s.c. or 5 mg/Kg by gavage, GW9662 25 mg/kg by gavage and Wy-14,643 100 mg/kg by gavage. Antagonists were given 30 min before injections of the corresponding agonists. Treatments were performed in the morning (10:00 a.m.) and photon detection was assayed 6 h later (4:00 p.m.).

MOL #42689

### **Bioluminescence reporter imaging.**

Mice were visualized with a Night Owl imaging unit (Berthold Technologies, Bad Wildbad, Germany) consisting of a Peltier cooled charge-coupled device slow-scan camera equipped with a 25 mmf/0.95 lens. Images were generated by a Night Owl LB981 image processor and transferred via video cable to a peripheral component interconnect (PCI) frame grabber using WinLight<sup>32</sup> software (Berthold Technologies, Bad Wildbad, Germany). For the detection of bioluminescence, mice were anesthetized using a s.c. injection of 50  $\mu$ l Ketamine-Xilazine solution composed by 78 % Ketamine (Ketavet 50, Intervet, Peschiera Borromeo, Italy), 15 % Xilazine (Rompun 2% solution, Bayer, Leverkusen, Germany), 7 % water and then received, if not otherwise specified in the text, i.p. injection of 25 mg/kg D-luciferin (25 mg/kg; Promega, Madison, WI, USA) 20 min before bioluminescence quantification, to obtain an uniform biodistribution of the substrate. We administered the substrate D-luciferin following a described procedure (Ma et al., 1993; Patrone et al., 1998). Mice were placed in the light-tight chamber and a grey scale photo of the animals was first taken with dimmed light. Photon emission was then integrated over a period of 5 min.

*Ex vivo* optical imaging assay was performed on dissected tissues. Animals were injected with 25 mg/kg luciferine and killed after 20 min; photon emission from each organ, kept in phosphate-saline buffer, was monitored over a period of 10 min with the Night Owl imaging unit as above described.

### **Luciferase enzymatic assay**

For enzymatic assay of luciferase activity, tissues from euthanized mice were dissected and immediately frozen on dry ice. Protein extracts were prepared by potter homogenization in 200  $\mu$ l of 100 mM KPO<sub>4</sub> lysis buffer (pH 7.8 containing 1 mM dithiothreitol, 4 mM EGTA, 4 mM EDTA, and 0.7 mM phenylmethylsulfonyl fluoride), three cycles of freezing-thawing, and 30 min of minifuge centrifugation (Eppendorf, Hamburg, Germany) at maximum speed. Supernatants containing luciferase were collected, and protein concentrations were determined by Bradford's

MOL #42689

assay (Bradford, 1976). Luciferase enzymatic activity was measured by a commercial kit (Luciferase assay system, Promega, Madison, WI, USA) according to the supplier's instructions. The light intensity was measured with a luminometer (Veritas, Promega, Madison, WI, USA) over a 10-sec time periods and expressed as relative light units per  $\mu\text{g}$  protein (RLU/  $\mu\text{g}$  protein).

### Real-Time PCR Gene Expression Analysis

Real-time PCR experiments were done with total RNAs extracted after tissues homogenization in TRIzol reagent (Invitrogen Corporation, Carlsbad, CA, USA) as suggested by the manufacturer's instructions. For the preparation of cDNA, 1  $\mu\text{g}$  RNA was denatured at 75 C for 5 min in the presence of 1.5  $\mu\text{g}$  of random primers (Promega) in 15  $\mu\text{l}$  final volume. Deoxynucleotide triphosphate (GE Healthcare, Piscataway, NJ) and Moloney murine leukemia virus reverse transcriptase (RT) (Promega) were added at 0.5 mM and 8 U/ $\mu\text{l}$  final concentration, respectively, in a final volume of 25  $\mu\text{l}$ . The RT reaction was performed at 37 C for 1 h; the enzyme was inactivated at 75 C for 5 min. Control reactions without addition of the RT enzyme were performed for each sample. Real-time PCR experiments were performed using TaqMan technology. The reaction mix for each sample was made up of 5  $\mu\text{l}$  of cDNA (1:25 dilution), 12.5  $\mu\text{l}$  of TaqMan 2x Universal PCR Master Mix No AmpErase UNG (Applied Biosystems, Foster City, CA) and 7.5  $\mu\text{l}$  of primers and probes mix: 300 nM *Abcd2* forward and reward primers (5'-TGGTGGCTTCCAGGCTAAAC-3', 5'-GGGACCAGTTATCAAGAGATGCA-3'), 200 nM *Abcd2* TaqMan MGB probe 5'-6FAM-TCAAAGTGGAAGAAGGG-MGB-3'; pre-made TaqMan Gene Expression assays for the endogenous gene *Acox1* (Mm00443579\_m1, Applied Biosystems), and as a reference gene assay 18S rRNA VIC-MGB-PDAR (Applied Biosystems). The reaction was carried out according to the manufacturer's protocol using Applied Biosystems 7000 Sequence Detection System device with the following thermal profile: 2 min at 50 C; 10 min 95 C; 40 cycles (15 s 95 C, 1 min at 60 C), and



MOL #42689

data were analyzed using the ABI Prism 7000 SDS Software and the  $2^{-\Delta\Delta Ct}$  method (Livak et al., 2001). The analysis of each sample was repeated six times.

### **HPLC analysis of drug amount in tissues**

The tissue samples (100 mg) were homogenized in 1.0 ml of ice cold Methanol using a Ultra-Turrax homogenizer (IKA Works inc. Wilmington, NC, USA). Complete homogenization took 30 s or less. The homogenates were centrifuged for 10 min at 3000 g at 4 C . The clear supernatant was directly injected onto HPLC system (Waters Alliance 2695 separation module with automatic injector set at +4°C; Waters Corporation, Milford, MA, USA)

Injection volume : 10 µl; Column: Symmetry 300TM C4 5 µm 125 x 4.6mm; Column flow rate: 1 ml/min; Mobile phase: 30% Water acidified with 0.1% formic acid 70% Methanol acidified with 0.1% formic acid; Split post-column: 1:8.

### **Statistical analysis**

Statistical analysis using GraphPad software (GraphPad Software Inc. San Diego, CA, USA) was performed using ANOVA followed by Bonferroni's test with the only exceptions of data shown in Figure 2, Figure 5 and Figure 7C where Student's t test was performed.

MOL #42689

## RESULTS

### Reporter mice: *in vivo* imaging of reporter gene expression.

In a luciferase-reporter mouse, *in vivo* evaluation of the potency of a given ligand to elicit luciferase expression, requires prior study of the diffusion to all organs of the enzyme substrate, D-luciferin, at a concentration sufficient to saturate the reporter enzymatic activity. Therefore, preliminary experiments were carried out to study the kinetics of D-luciferin distribution and to define the dose sufficient to fully activate the luciferase produced in the different tissues. To establish the dynamics of D-Luciferin diffusion, PPRE-*Luc* mice were injected i.p. with 79.2 mg/kg of D-luciferin and photon emission was quantified, as described in the methodology section, with a sequence of Charge-Coupled Device-camera (CCD-camera) sessions of 5 min each. Figure 1A shows that in chest photon emission was maximal between 10 and 25 min after the i.p. injection and then gradually decreased. The result was consistent with previous observations made in another reporter model, the ERE-*Luc* mouse, where the CCD-camera sessions were carried out only for 30 min after i.p. injection of the same dose of D-luciferin (79.2 mg/kg). In the ERE-*Luc* mouse model, we could evaluate photon emission from chest and abdomen: in both areas maximal luciferase activity was measured between 10 to 15 min, then the emission did not change up to 30 min (Fig. 1B). We concluded that observations made between 20 and 25 min guaranteed the optimal distribution of the substrate to the different tissues. This window of time was therefore selected for future experiments. Next, we injected PPRE-*Luc* mice with 8.8; 17.6; 26.5; and 79.2 mg/kg of D-luciferin. Figure 1C shows that at 20 min after injection, the highest dose of substrate (79.2 mg/kg) determined maximal bioluminescence emission. Once more, the results were superimposable with those of previous studies with ERE-*Luc* mice where we considered three different doses of luciferin (8.8; 26.5; 79.2 mg/kg, i.p. injection) (Fig. 1D) and observed maximal bioluminescence with the dose of substrate 79.2 mg/kg. However, because of the toxicity of repeated treatments particularly when animals were repeatedly anaesthetized, the dose of 26.5 mg/kg had to be used, particularly in chronic studies.

MOL #42689

Present technology for bioluminescence-based *in vivo* imaging can be consistently carried out in reporter mice only in two dimensions, thus the definition of the organ/tissue contributing to the photon emission as measured *in vivo* is limited; furthermore, signaling from the most inner organs is significantly reduced by photon scattering and absorption by the tissues crossed by the photons. Therefore, to better evaluate the homogeneous diffusion of D-luciferin, we carried out a series of *ex vivo* experiments where we measured luciferase activity of organs dissected from the mice euthanized at different times after i.p. injection of D-luciferin (26.5 mg/kg). The measurement of the enzyme activity was done first by bioluminescence (Fig. 2, A and B), exposing the dissected organ to the CCD camera, then the organ was rapidly frozen for the preparation of tissue extracts where luciferase enzymatic activity was measured (Fig. 2C). Luciferase activity, as assessed by enzymatic assay in the tissue extracts, provided results superimposable with CCD-camera quantitative experiments.

The *ex vivo* experiments were carried out also on animals pretreated with a pharmacological dose (50 mg/kg) of the PPAR $\alpha$  agonist Wy-14,643 or vehicle to ensure that the concentration of D-luciferin substrate was adequate for the quantitative measurement of the large amount of luciferase accumulating shortly after stimulation of PPARs. Figure 2 shows the intensity of signaling by isolated organs before and after the pharmacological treatment as measured by bioluminescence (Fig. 2, A and B) or by enzymatic assay (Fig. 2C) in tissue extracts. In Wy-14,643 *versus* vehicle treated mice, optical imaging and enzymatic assay showed a significant increase of luciferase activity in liver. High variability in the response was observed in testis and heart where, as clearly shown by the imaging data, only a minute amount of cells was responsive to the treatment with the PPAR $\alpha$  agonist. In brain luciferase activity was unaffected by the treatment. To verify the reliability of the reporter used in the study, we next measured by real time PCR the accumulation of *Acyl-CoA oxidase1, palmitoyl (Acox1)*, a well known PPAR $\alpha$  target gene (Stauber et al., 2005), (Figure 2D). *Acox1* mRNA was significantly increased in liver and, similarly to what shown with luciferase this mRNA appeared to be slightly increased in testis and perhaps in heart, but not in

MOL #42689

brain. HPLC measurements of Wy-14,643 content in the various organs showed that the ligand was maximally concentrated in liver and reached heart and, to lower extent, testis; no brain penetration of the compound was observed (Fig. 2E). These data on drug distribution were consistent with the observed induction of luciferase activity.

### **PPRE-*Luc* mouse in pharmacological analysis.**

To test the ability of PPRE-*Luc* mouse to identify molecules active on all PPAR subtypes, we treated adult male PPRE-*Luc* mice with a series of isoform-specific ligands such as the PPAR $\alpha$  agonist Wy-14,643 (250 mg/kg s.c.), the PPAR $\gamma$  agonists Rosiglitazone (50 mg/kg s.c.) and GW1929 (50 mg/kg by gavage) and the PPAR $\beta/\delta$  agonist GW501516 (50 mg/kg by gavage). We also tested two novel compounds (Dell'Uomo et al., 2006): a dual, PPAR $\alpha$ -PPAR $\gamma$  agonist, ST2518 (250 mg/kg s.c.) and a PPAR $\alpha$  selective agonist ST1929 (250 mg/kg s.c.). Controls were treated with vehicle (oil for s.c. treatments or 0.5% carbosimetilcellulose (CMC) water solution for gavage treatments). Each mouse was subjected to a CCD-camera session at 0, 3, 6 and 24 h after treatment (Fig. 3). Interestingly, the kinetics of the onset of bioluminescence emission were very similar with all compounds tested and were not modified by the route of administration selected for each compound. The highest photon emission was always observed 6 h after treatment and was indistinguishable from controls at 24 h with the only exception of ST2518. This indicates that the activity on PPARs of all ligands, but ST2518, was back to unstimulated levels 24 h after administration possibly due to the fact that ST2518 was less readily catabolized.

These kinetics of nuclear receptor activity in response to treatment are in line with previous studies on the ERE-*Luc* reporter mouse by ours (Ciana et al., 2001; Ciana et al., 2003; Maggi et al., 2004) as well as other groups (Lemmen et al., 2004) and are supported by the analysis of the hormonal treatment of endogenous genes (Di Lorenzo et al. in preparation). It is important to underline that the use of firefly luciferase, a protein with a turnover rate of 2-3 h, was instrumental to show the cessation of drug action; this would have not been possible with the use of more stable reporters

MOL #42689

which would have maintained their activity after cessation of receptor activation. The PPAR $\alpha$  agonist induced the highest photon emission in chest, as expected on the basis of the high expression of this PPAR receptor subtype in liver; in line with the receptor expression PPAR $\gamma$ , PPAR $\beta/\delta$  and PPAR $\alpha$  agonists induced luciferase production in abdomen and chest; in fact it is well known that all PPARs are expressed in the digestive tract. The new compound ST1929 (PPAR $\alpha$  agonist) induced, but not to a significant extent, maximal luciferase activity in chest at 6 h, however, we also observed an activity in abdomen which was still high at 24 h.

To better evaluate the extent to which in PPRE-*Luc* mouse the reporter activity reflected the intensity of the signaling on the receptor, we investigated the effect of 6 h treatment with 10 and 50 mg/kg s.c. of rosiglitazone (PPAR $\gamma$ ) agonist and 50 and 250 mg/kg s.c. of the PPAR $\alpha$  agonist Wy-14,643 (Fig. 4). Both *in vivo* imaging (Fig. 4A) and luciferase enzymatic assay in tissue extracts (Fig. 4B) showed a clear effect of the dosage. Wy-14,643, a PPAR $\alpha$  agonist, was active in liver and heart, while the PPAR $\gamma$  agonist rosiglitazone was active in liver, intestine and adipose tissue (PRAT; Peri Renal Adipose Tissue, that is mixed white and brown adipose tissue), but not in heart: a tissue not expressing PPAR $\gamma$ . The use of selective antagonists both for PPAR $\alpha$  (MK-886, 250 mg/kg s.c.) (Kehrer et al., 2001) and PPAR $\gamma$  (GW9662; 50 mg/kg s.c.) (Leesnitzer et al., 2002) further demonstrated the reliability of the reporter in showing their ability to block the agonist effect on each PPAR subtype. The PPAR $\alpha$  antagonist MK-886 significantly reduced luciferase activity in the heart, indicating that PPAR $\alpha$ -dependent transcription is constitutively activated in this tissue in untreated condition; the high basal level of transcription seems to preclude further receptor activation after Wy 14,643 administration (Figure 4B).

The antagonist activity of GW9662 in PRAT was further demonstrated on animals subjected to the treatment for a prolonged period of time (Fig. 4C).

**Prolonged treatment with the PPAR $\alpha$  selective agonist Wy-14,643 affects receptor signaling.**

MOL #42689

*In vivo* imaging offers the opportunity to evaluate the effect of a repetitive treatments in the same animal, thus providing a view on the response of the receptor system to the treatment in time. To evaluate the effect of prolonged treatments with a selective PPAR $\alpha$  agonist, Wy-14,643 was administered daily at 100 mg/kg/d by gavage for 21 d (Fig. 5A). Most interestingly, during the treatment, the state of transcriptional activity of liver PPAR $\alpha$  receptor changed significantly. In the first 5 d of treatment, liver PPAR $\alpha$  activity was most stimulated (up to 8-10 fold higher than controls), but the ability of the agonist to trigger the receptor activity appeared to decrease with time. The results of the *in vivo* imaging data (Fig. 5A), calculated as area under the curve (Fig. 5B), during the first 5 d of treatment or during the entire treatment, were confirmed in a subsequent study where luciferase activity was measured in liver tissue extracts of animals euthanized after 5 or after 21 d of continuous treatment (Fig. 5C).

The negative peaks observed every 6-7 d in the graph reporting the daily activity of the PPARs lead to speculate the possibility of a cyclic desensitization of the receptor in response to continuous stimulation.

The study led us to conclude that reporter animals enable to study the effect of a given drug on its target during time: this ability might provide clues instrumental to optimize dosages and treatment schedules ensuring the maximal effects at the lowest dosage. For instance, the results of our experiment would suggest that a discontinuous administration with Wy-14,643 might result in a persistent receptor activity in time; thus a more effective treatment with a reduced exposure to the drug.

### **Screening of PPAR activity of novel molecules.**

A dose-response study was also carried out in male PPRE-*Luc* mice for the two novel PPAR agonists: ST2518 shown, in cell transactivation assay, to possess a PPAR $\alpha$  and PPAR $\gamma$  dual-agonist activity and ST1929 shown to be a PPAR $\alpha$  agonist. Two different dosages of 50 and 250 mg/kg, s.c. were used; 6 h after treatment with ST2518, *in vivo* optical imaging analysis revealed a significant

MOL #42689

luciferase induction in chest and abdomen; no effect was detectable in the testis with both compounds (Fig. 6, A and B). The enzymatic assay (Fig. 6C) confirmed a significant induction of PPARs in liver with ST2518 and a trend to increase with ST1929 treatment. In the heart, the high background in the control group (Ciana et al., 2007), prevented the observation of a clear effect of the agonist: indeed only a trend to induction of luciferase expression by agonists was measured. The lack of a clear dose-dependent effect on luciferase expression indicated that the lower dose of compound used was sufficient to reach maximum receptor activation. Previous transactivation studies (Dell'Uomo et al., 2006), carried out using the PPAR $\alpha$ <sub>LBD</sub>-GAL4 or PPAR $\gamma$ <sub>LBD</sub>-GAL4 fusion proteins, showed a comparable efficacy of the two ligands on PPAR $\alpha$  (ST1929, methyl estere of the para isomer ST2518: EC50 31.9  $\mu$ M, efficacy 6.8 fold as compared to fenofibrate, data not shown; ST2518: EC50 5,63  $\mu$ M, efficacy 7.7 fold as compared to fenofibrate). Thus, the *in vivo* comparison between ST1929 and ST2518 ability to transactivate PPAR $\alpha$  in the liver of PPRE-*Luc* mice (Fig. 6) shows that the comparable efficacy of the two compounds detected by *in vitro* studies represent an overestimation of the real potency that ST1929 compound has in the liver of living mice.

### **PPRE-*Luc* reporter mouse reveals a remarkable SPPARM activity in testis and lung.**

The *in vivo* imaging analysis of mice treated with PPAR $\alpha$  ligands showed that in testis the selective antagonist MK-886 did not block the agonist Wy-14,643 activity, but, instead, significantly increased it. Furthermore, MK-886 alone induced a highly significant increase of photon emission (Fig. 7A). Additional studies on a wider number of organs of luciferase activity in tissue extracts supported the finding and showed that, when administered alone, MK-886 specifically induces luciferase activity in testis and in lungs (Fig. 7B) and the effect is not additive when MK-886 is administered in combination with Wy-14,643

The results obtained both by *in vivo* imaging and enzymatic assay were confirmed by the analysis of the expression of endogenous genes done by real time PCR. Fig 7C shows that MK-886 induced

MOL #42689

*ATP-binding cassette, subfamily D, member 2 (Abcd2)* and *Acox1* expression in lung; in testis the changes subsequent to the treatment were limited to the *Abcd2* mRNA. The lack of activation of *Acox1* might be due to the fact that this gene is not induced by PPAR $\alpha$  activation in this organ. Alternatively, the multifactorial control of *Acox1* promoter might limit the analysis of the effect of PPAR $\alpha$  ligands at least in testis. These data indicates that for the pharmacological analysis of PPAR modulators, reporter gene assay in vivo has a higher predictive power than the measurement of endogenous target genes: indeed reporter synthesis in the PPRE-*Luc* is controlled by a simple promoter where PPAR has a predominant role, whereas the activity of a complex promoter in a natural target gene context is susceptible of a series of input which may minimize the contribution of the PPAR activity.

Yet the data on luciferase and endogenous target gene expression are supporting each other in demonstrating a SPPARM activity of MK-886. To the best of our knowledge this is the first report of a SPPARM activity of this PPAR ligand. It is however important to underline that in addition to its ability to bind PPAR $\alpha$ , MK-886 was reported to inhibit 5-lipoxygenase-activating protein and thus to reduce the activity of the lipoxigenase enzymes. This inhibition has the potential to alter the levels of endogenous PPAR ligands; therefore it remains to be established the extent to which the PPAR $\alpha$  activation observed in testis and lung after MK-866 treatment is due to a local production of a specific ligand or to a direct binding activity of the compound on the receptor leading to a tissue specific recruitment of a co-activator complex.



MOL #42689

## DISCUSSION

The present study shows the power of reporter mouse technology when applied to pharmacological profiling of drugs active on intracellular receptors. For the first time, the introduction of a surrogate marker offers the possibility to directly titrate the action of a drug on its target in space and time avoiding extrapolations based on drug distribution parameters. The advantages of the reporter mice over the methods currently in use for preclinical drug development are several and can be summarized as follows: *i*) global view of the tissues affected by the treatment that enables a rapid identification of unexpected, potentially undesired, effects; *ii*) unequivocal, on target, assessment of dosage and timing necessary to elicit the pharmacological response; *iii*) possibility to carry out longitudinal studies in single individuals during repeated drug treatment to unravel sites of drug accumulation and activity, or the dynamics of the target response to the treatment (e.g. receptor desensitization or down/up-regulation); *iv*) possibility to perform time-course studies with limited use of experimental animals.

The present study exemplifies all of the above concepts. First, it demonstrates the importance of *in vivo* analysis to obtain a global view of the drug effects by describing a novel activity of the PPAR $\alpha$  antagonist MK-886. It is in fact well known that compounds acting on NR may act as antagonists in a set of cells and, in others, be agonists. This mixed activity was first described for drugs such as Tamoxifen or Raloxifene and named Selective Estrogen Receptor Modulators (Katzenellenbogen, 1996; Jordan, 2001; Wu et al., 2005; Swaby et al., 2007). The “selective” modulation of NR is due to NR interaction with tissue-specific co-regulators that modulate NR ability to induce transcription of target genes (McKenna et al., 1999; Robyr et al., 2000; O'Malley, 2007). The current method to identify NR ligands with mixed agonist/antagonist action is based on the screening of their activity in a series of reporter cells of different tissue origin, often even using synthetic receptors (such as NR<sub>LBD</sub>-GAL4 fusion protein) unable to correctly interact with co-regulators. Our *in vivo* data show that ligands believed to have similar efficacy *in vitro* indeed behave quite differently when studied in reporter mice (Fig. 6). This may be ascribed to differential molecular interactions in the target

MOL #42689

cells or differential adsorption or distribution. In the present study, the limits of *in vitro* studies are underlined by the fact that they failed to identify the SPPARM activity of MK-886 clearly shown by *in vivo* imaging using the PPRE-*Luc* mouse model (Fig. 7).

Second, the pharmacological studies here reported illustrate the supremacy of animal reporter systems for the definition of the kinetics of drug action. The observation that all compounds had a peak of activity at 6 h is intriguing: however, due to the high lipophilic profile shared by all compounds, it is possible that all have a very similar kinetics of distribution to the different tissues; on the other hand, the finding that ST2518, differs from all other compounds maintaining its activity for 24 h, indicates that the reporter system may reveal compounds not readily metabolized or excreted (Fig. 3). In previous studies (Ciana et al., 2003; Ciana et al., 2007), we have shown that luciferase activity mirrors the transcriptional activity of the receptor on endogenous target genes. However, the use of endogenous target genes as marker of PPAR activation may lead to conflicting results due to the complexity of endogenous promoters. It is important to stress that the simple PPRE-tk promoter driving luciferase expression in the PPRE-*Luc* model simplifies significantly the analysis of drug activity in the different tissues eliminating the interference of other transcription regulators, typically acting on the endogenous complex promoters, and leading to ambiguous interpretation on the state of activity of the receptor. A possible drawback for the use of the PPRE-*Luc* reporter mouse is the limited possibility to discriminate which subtype of PPARs is actually contributing to the luciferase expression; however, this problem may be overcome by breeding the model with subtype-specific knock out models or using selective antagonists.

Finally, non invasive imaging methodologies facilitate the investigation of drug action when the treatment is continued in time. This is of major interest in developing drugs to be used chronically: as here shown, the daily examination of the effect of Wy-14,643 administration in individual animals reveals a dynamic response resulting in lowering the drug effect with time (Fig. 5). The analysis of such a response may be crucial for the definition of a timing of compound administration which elicits the highest response at the lowest dosage. In addition, the longitudinal

MOL #42689

study enables to identify sites more susceptible to the effect of the drug due to local accumulation of the drug or to the absence of physiological protective mechanism of feed-back.

Potential limitations of the current *in vivo* technology are a poor high-throughput and the two-dimensional imaging. The progress in the imaging field like 3D-CCD camera or the development of novel and more powerful reporter proteins for optical imaging (new luciferase mutant protein with a photon emission more shifted in the red spectrum), and for positron emission tomography will soon overcome present restrictions, yet, the use of *ex vivo* analysis provides a powerful methodology for the detailed study of the effects of large number of compounds. The reliability of imaging technology in isolated organs is here demonstrated by measuring luciferase enzymatic activity or photon emission in selected organs (Fig. 2). Thus *ex vivo* imaging could represent a very useful methodology for the precise and rapid measurement of the time frame and dosage necessary to elicit a pharmacological response or the accessibility of the drug to a given organ (e.g. brain).

In the last twenty years we witnessed major changes in drug research programs with a progressive adoption of “*in silico*” and cellular approaches driven by the cost/effectiveness of these methodologies and by the global pressure to limit the use of experimental animals. However, animal engineering by providing novel disease models is giving a new impetus to bio-medical research facilitating the understanding of the normal functioning of molecules, cells, organ systems and whole organisms and the changes induced by different pathologies. The use of reporter systems in disease models will certainly have an invaluable effect for the development and assessment of novel therapies, for the biological characterization of the disease and response to the drug, to titrate drug to disease response in tissues for accurate dosing and to determine whether the drug modifies the biological disease process or restores a normal process affected by disease with a dramatic improvement in the generation of novel and more efficacious drugs.

MOL #42689

## **ACKNOWLEDGMENTS**

We thank Cristina Martelli, Clara Meda, Balaji Ramachandran, Monica Rebecchi and Alessandro Peschechera for their technical assistance. We acknowledge the veterinarian support of Paolo Sparaciari all through the study.

MOL #42689

## REFERENCES

- Albet S, Causeret C, Bentejac M, Mandel JL, Aubourg P and Maurice B (1997) Fenofibrate differently alters expression of genes encoding ATP-binding transporter proteins of the peroxisomal membrane. *FEBS Lett* **405**:394-7.
- Anghel SI and Wahli W (2007) Fat poetry: a kingdom for PPARgamma. *Cell Res* **17**:486-511.
- Berger J and Moller DE (2002) The mechanisms of action of PPARs. *Annu Rev Med* **53**:409-35.
- Berger JP, Akiyama TE and Meinke PT (2005) PPARs: therapeutic targets for metabolic disease. *Trends Pharmacol Sci* **26**:244-51.
- Bradford MM (1976) A rapid and sensitive method for the quantitation of microgram quantities of protein utilizing the principle of protein-dye binding. *Anal Biochem* **72**:248-54.
- Ciana P, Di Luccio G, Belcredito S, Pollio G, Vegeto E, Tatangelo L, Tiveron C and Maggi A (2001) Engineering of a mouse for the in vivo profiling of estrogen receptor activity. *Mol Endocrinol* **15**:1104-13.
- Ciana P, Raviscioni M, Mussi P, Vegeto E, Que I, Parker MG, Lowik C and Maggi A (2003) In vivo imaging of transcriptionally active estrogen receptors. *Nat Med* **9**:82-6.
- Ciana P, Biserni A, Tatangelo L, Tiveron C, Sciarroni AF, Ottobrini L and Maggi A (2007) A novel peroxisome proliferator-activated receptor responsive element-luciferase reporter mouse reveals gender specificity of peroxisome proliferator-activated receptor activity in liver. *Mol Endocrinol* **21**:388-400.
- Conner P (2007) Breast response to menopausal hormone therapy--aspects on proliferation, apoptosis and mammographic density. *Ann Med* **39**:28-41.
- Dell'Uomo N, Tassoni E, Brunetti T, Pessotto P, Sciarroni AF, Milazzo FM, De Angelis F, Peschechera A, Tinti MO, Carminati P and Giannessi F (2006) 2-{3-[2-(4-chlorophenyl)ethoxy]phenylthio}-2-methylpropanoic acid: a fibrate-like compound with hypolipidemic and antidiabetic activity. *ChemMedChem* **1**:49-53.
- Evans RM, Barish GD and Wang YX (2004) PPARs and the complex journey to obesity. *Nat Med*

MOL #42689

**10**:355-61.

Fruchart JC, Duriez P and Staels B (1999) Peroxisome proliferator-activated receptor-alpha activators regulate genes governing lipoprotein metabolism, vascular inflammation and atherosclerosis. *Curr Opin Lipidol* **10**:245-57.

Gale EA (2001) Lessons from the glitazones: a story of drug development. *Lancet* **357**:1870-5.

Graham DJ, Green L, Senior JR and Nourjah P (2003) Troglitazone-induced liver failure: a case study. *Am J Med* **114**:299-306.

Home PD, Pocock SJ, Beck-Nielsen H, Gomis R, Hanefeld M, Jones NP, Komajda M and McMurray JJ (2007) Rosiglitazone evaluated for cardiovascular outcomes--an interim analysis. *N Engl J Med* **357**:28-38.

Jordan VC (2001) Selective estrogen receptor modulation: a personal perspective. *Cancer Res* **61**:5683-7.

Katzenellenbogen JA, O'Malley BW and Katzenellenbogen BS (1996) Tripartite steroid hormone receptor pharmacology: interaction with multiple effector sites as a basis for the cell- and promoter-specific action of these hormones. *Mol Endocrinol* **10**:119-31.

Kehrer JP, Biswal SS, La E, Thuillier P, Datta K, Fischer SM and Vanden Heuvel JP (2001) Inhibition of peroxisome-proliferator-activated receptor (PPAR)alpha by MK886. *Biochem J* **356**:899-906.

Kliwer SA, Umesono K, Noonan DJ, Heyman RA and Evans RM (1992) Convergence of 9-cis retinoic acid and peroxisome proliferator signalling pathways through heterodimer formation of their receptors. *Nature* **358**:771-4.

Kostadinova R, Wahli W and Michalik L (2005) PPARs in diseases: control mechanisms of inflammation. *Curr Med Chem* **12**:2995-3009.

Kota BP, Huang TH and Roufogalis BD (2005) An overview on biological mechanisms of PPARs. *Pharmacol Res* **51**:85-94.

Lazarenko OP, Rzonca SO, Hogue WR, Swain FL, Suva LJ and Lecka-Czernik B (2007)

MOL #42689

- Rosiglitazone induces decreases in bone mass and strength that are reminiscent of aged bone. *Endocrinology* **148**:2669-80.
- Leesnitzer LM, Parks DJ, Bledsoe RK, Cobb JE, Collins JL, Consler TG, Davis RG, Hull-Ryde EA, Lenhard JM, Patel L, Plunket KD, Shenk JL, Stimmel JB, Therapontos C, Willson TM and Blanchard SG (2002) Functional consequences of cysteine modification in the ligand binding sites of peroxisome proliferator activated receptors by GW9662. *Biochemistry* **41**:6640-50.
- Lehmann JM, Moore LB, Smith-Oliver TA, Wilkison WO, Willson TM and Kliewer SA (1995) An antidiabetic thiazolidinedione is a high affinity ligand for peroxisome proliferator-activated receptor gamma (PPAR gamma). *J Biol Chem* **270**:12953-6.
- Lemmen JG, Arends RJ, van Boxtel AL, van der Saag PT and van der Burg B (2004) Tissue- and time-dependent estrogen receptor activation in estrogen reporter mice. *J Mol Endocrinol* **32**:689-701.
- Livak KJ and Schmittgen TD (2001) Analysis of relative gene expression data using real-time quantitative PCR and the 2(- $\Delta\Delta C_t$ ) method. *Methods* **25**:402-408
- Ma ZQ, Spreafico E, Pollio G, Santagati S, Conti E, Cattaneo E and Maggi A (1993) Activated estrogen receptor mediates growth arrest and differentiation of a neuroblastoma cell line. *Proc Natl Acad Sci U S A* **90**:3740-4.
- Maggi A, Ottobriani L, Biserni A, Lucignani G and Ciana P (2004) Techniques: reporter mice - a new way to look at drug action. *Trends Pharmacol Sci* **25**:337-42.
- Masubuchi Y (2006) Metabolic and non-metabolic factors determining troglitazone hepatotoxicity: a review. *Drug Metab Pharmacokinet* **21**:347-56.
- McKenna NJ, Lanz RB and O'Malley BW (1999) Nuclear receptor coregulators: cellular and molecular biology. *Endocr Rev* **20**:321-44.
- Nissen SE and Wolski K (2007) Effect of rosiglitazone on the risk of myocardial infarction and death from cardiovascular causes. *N Engl J Med* **356**:2457-71.

MOL #42689

O'Malley BW (2007) Coregulators: from whence came these "master genes". *Mol Endocrinol* **21**:1009-13.

Patrone C, Gianazza E, Santagati S, Agrati P and Maggi A (1998) Divergent pathways regulate ligand-independent activation of ER alpha in SK-N-BE neuroblastoma and COS-1 renal carcinoma cells. *Mol Endocrinol* **12**:835-41.

Psaty BM and Furberg CD (2007) The record on rosiglitazone and the risk of myocardial infarction. *N Engl J Med* **357**:67-9.

Pujol A, Ferrer I, Camps C, Metzger E, Hindelang C, Callizot N, Ruiz M, Pampols T, Giros M and Mandel JL (2004) Functional overlap between ABCD1 (ALD) and ABCD2 (ALDR) transporters: a therapeutic target for X-adrenoleukodystrophy. *Hum Mol Genet* **13**:2997-3006.

Rampler H, Weinhofer I, Netik A, Forss-Petter S, Brown PJ, Oplinger JA, Bugaut M and Berger J (2003) Evaluation of the therapeutic potential of PPARalpha agonists for X-linked adrenoleukodystrophy. *Mol Genet Metab* **80**:398-407.

Reeves GK, Beral V, Green J, Gathani T and Bull D (2006) Hormonal therapy for menopause and breast-cancer risk by histological type: a cohort study and meta-analysis. *Lancet Oncol* **7**:910-8.

Robyr D, Wolffe AP and Wahli W (2000) Nuclear hormone receptor coregulators in action: diversity for shared tasks. *Mol Endocrinol* **14**:329-47.

Rosen ED, Walkey CJ, Puigserver P and Spiegelman BM (2000) Transcriptional regulation of adipogenesis. *Genes Dev* **14**:1293-307.

Rzonca SO, Suva LJ, Gaddy D, Montague DC and Lecka-Czernik B (2004) Bone is a target for the antidiabetic compound rosiglitazone. *Endocrinology* **145**:401-6.

Shi GQ, Dropinski JF, McKeever BM, Xu S, Becker JW, Berger JP, MacNaul KL, Elbrecht A, Zhou G, Doebber TW, Wang P, Chao YS, Forrest M, Heck JV, Moller DE and Jones AB (2005) Design and synthesis of alpha-aryloxyphenylacetic acid derivatives: a novel class of



MOL #42689

- PPAR $\alpha$ /gamma dual agonists with potent antihyperglycemic and lipid modulating activity. *J Med Chem* **48**:4457-68.
- Stauber AJ, Brown-Borg H, Liu J, Waalkes MP, Laughter A, Staben RA, Coley LC, Swanson C, Voss KA, Kopchick JJ and Corton JC (2005) Constitutive Expression of Peroxisome Proliferator-Activated Receptor  $\alpha$ -Regulated Genes in Dwarf Mice. *Mol Pharmacol* **67**:681–694.
- Swaby RF, Sharma CG and Jordan VC (2007) SERMs for the treatment and prevention of breast cancer. *Rev Endocr Metab Disord*.
- Tugwood JD, Issemann I, Anderson RG, Bundell KR, McPheat WL and Green S (1992) The mouse peroxisome proliferator activated receptor recognizes a response element in the 5' flanking sequence of the rat acyl CoA oxidase gene. *Embo J* **11**:433-9.
- Watkins PB and Whitcomb RW (1998) Hepatic dysfunction associated with troglitazone. *N Engl J Med* **338**:916-7.
- Woolf AD (2007) An update on glucocorticoid-induced osteoporosis. *Curr Opin Rheumatol* **19**:370-5.
- Wu YL, Yang X, Ren Z, McDonnell DP, Norris JD, Willson TM and Greene GL (2005) Structural basis for an unexpected mode of SERM-mediated ER antagonism. *Mol Cell* **18**:413-24.

MOL #42689

## FOOTNOTES

The study was supported by Sigma-Tau Industrie Farmaceutiche Riunite S.p.A., Telethon GGP02336, the European Community (NoE DIMI (LSHB-CT-2005-512146), NoE EMIL (LSHC-CT-2004-503569), IP CRESCENDO (LSHM-CT-2005-018652) and EPITRON (LSHC-CT-2005-518417) Strep EWA (LSHM-CT-2005-518245) and NIH (R01AG027713-02).

MOL #42689

## FIGURE LEGENDS

### Figure 1. Biodistribution of luciferase substrate in reporter mice.

A-B, optical imaging and photon counting of the luciferase activity of male PPRE-*Luc* and ERE-*Luc* mice i.p. injected with 79.2 mg/kg D-luciferin. Photon emission (counts *per second*; cts/s) was quantified in selected body areas by a series of 5 min CCD-camera acquisitions in each animal. C-D, PPRE-*Luc* and ERE-*Luc* male mice were injected with different doses of D-luciferin (PPRE-*Luc*: 8.8, 17.6, 26.4 and 79.2 mg/kg; ERE-*Luc*: 8.8, 26.4 and 79.2 mg/kg) for 20 min. Photon emission was quantified for 5 min within the indicated body areas. Images show acquisition of a single representative animal and all data represent the mean  $\pm$  S.E.M. of acquisitions made in groups of five-ten animals. Photon emission was quantified using an electronic grid as shown in panel A: grid n°1 and 2 delimitate the areas named chest and abdomen.

### Fig. 2 - *Ex vivo* evaluation of the luciferase activity.

PPRE-*Luc* male mice were treated s.c. with 50 mg/kg Wy-14,643 or vehicle and euthanized after 6 h. Organs were rapidly dissected for imaging (A) and photon counting (B) and then frozen for subsequent luciferase analysis by enzymatic assay (C). Luciferase activity was measured by enzymatic assay on protein extracts and expressed as Relative Light Unit for  $\mu$ g of proteins (RLU/ $\mu$ g protein). D, The expression of the endogenous PPAR $\alpha$  target gene, *Acox1*, was determined by semiquantitative real-time PCR carried on total mRNA extracted from the indicated tissues.. E, Measurement of the total amount of Wy-14,643 in brain (red plot), heart (black plot), testis (blue plot) and liver (green plot) was performed by HPLC at 1, 2, 3, 6 and 24h after Wy-14,643 treatment (s.c. 50 mg/kg) and expressed as  $\mu$ g Wy-14,643 / g tissue. Bars represent mean  $\pm$  SEM of five mice. \*,  $P < 0.05$  and \*\*,  $P < 0.005$  as compared with vehicle treatment. P values were calculated by t test. The experiment was repeated three times.

MOL #42689

**Fig. 3 – Time course of the Luciferase activity in PPRE-*Luc* mice after treatment with synthetic PPAR agonists.**

PPRE-*Luc* mice were treated with Wy-14,643 (PPAR $\alpha$  agonist; 250 mg/kg s.c.), Rosiglitazone (PPAR $\gamma$  agonist; 50 mg/kg s.c.), GW1929 (PPAR $\gamma$  agonist; 50 mg/kg by gavage), GW501516 (PPAR $\beta/\delta$  agonist; 50 mg/kg by gavage), ST2518 (PPAR $\alpha$  and PPAR $\gamma$  dual-agonist; 250 mg/kg s.c.) and ST1929 (PPAR $\alpha$  agonist; 250 mg/kg s.c.) or vehicle (vegetal oil for s.c. treatments or 0.5% CMC water solution for gavage treatments). Photon emission in chest and abdomen was measured at 0, 3, 6 and 24 h after treatment. In the left panels individual animals, each representative of an experimental group, are shown. Bars represent the mean  $\pm$  S.E.M. of at least five mice. \*,  $P < 0.05$ ; \*\*  $P < 0.01$  \*\*\*,  $P < 0.001$  *versus* time 0. P values were calculated with ANOVA followed by Bonferroni's test. The experiment was repeated twice.

**Fig. 4 – Modulation of Luciferase activity in the PPRE-*Luc* reporter mouse after treatment with selective agonists and antagonists of PPAR $\alpha$  and PPAR $\gamma$ .**

Groups of at least five PPRE-*Luc* male mice were treated for 6 h s.c. with vehicle (vegetal oil, white bars) or the indicated doses of PPAR $\alpha$  (Wy-14,643) and PPAR $\gamma$  (Rosiglitazone) agonists at the following doses: 50 mg/kg Wy-14,643 (W50, bright blue bars) or 250 mg/kg (W250, dark blue bars); 10 mg/kg Rosiglitazone (R10, bright green bars) or 50 mg/kg (R50 dark green bars). Antagonists, 250 mg/kg MK-886 (PPAR $\alpha$ ) and 50 mg/kg GW9662 (PPAR $\gamma$ ), were administered 30 min before s.c. injection of the lower dose of Wy-14,643 (W50+M250, bright blue striped bars) and Rosiglitazone (R10+G50, bright green striped bars). A, Optical imaging of a representative PPRE-*Luc* mouse, left, and relative quantification of photon emission in chest and abdomen, right. B, *Ex vivo* luciferase activity in liver and heart protein extracts after 6 h treatment with PPAR $\alpha$  ligands (upper panel) and in liver, heart, intestine and PRAT (Peri Renal Adipose Tissue) of mice treated with PPAR $\gamma$  ligands (lower panel). C, Luciferase enzymatic activity on PRAT total protein extracts of mice treated for 10 d by gavage with vehicle (0.5% CMC water solution, white bars),

MOL #42689

Rosiglitazone (5 mg/kg; R5, green bars) and 25 mg/kg GW9662 given 30 min before 5 mg/kg Rosiglitazone (R5+G25, green striped bars). Luciferase activity is expressed as Relative Light Unit for  $\mu\text{g}$  of proteins (RLU/ $\mu\text{g}$  protein). Bars represent the mean  $\pm$  S.E.M. of five mice. \*,  $P < 0.01$  and \*\*,  $P < 0.005$  as compared with 6 h vehicle treatment; °,  $P < 0.01$  as compared with the W50 treatment; \*\*\*,  $P < 0.001$  as compared with 6 h vehicle treatment.  $\Delta$ ,  $P < 0.05$  as compared with 6 h R10 treatment. #,  $P < 0.05$  as compared with vehicle treatment; §,  $P < 0.05$  as compared with the R5 treatment; P values were calculated with ANOVA followed by Bonferroni's test. The experiment was repeated twice.

**Fig. 5 - Imaging of PPAR $\alpha$  activation in PPRE-*Luc* reporter mice after repeated administration of Wy-14,643.**

Groups of five reporter mice were treated daily, for 21 d, with an oral dose of 100 mg/kg Wy-14,643 (filled square) or vehicle (0.5% CMC water solution, open square). A, photon emissions (cts/s) measured in the chest area each day at 4:00 p.m. (6 h after treatment) were averaged and plotted. B, The graph represents the area under the curve values calculated for the 1-5 d and for the entire treatment (1-21 d) on the basis of cts/s measured daily in animals treated with vehicle (red bar) or Wy-14,643 (blue bar). C, Luciferase activity was measured in protein extracts from the liver of mice that received the treatment for 5 and 21 d. Bars represent the mean  $\pm$  S.E.M. of five mice. \*,  $P < 0.05$  *versus* vehicle; Bars represent the mean  $\pm$  S.E.M. of 5 mice. P values were calculated by t test. RLU, Relative light units. The experiment was repeated twice with superimposable results.

**Fig. 6 - The profile of PPAR activation in living mice elicited by ST2518 and ST1929, two novel PPAR ligands.**

Groups of five reporter mice were s.c. treated with 50 mg/kg or 250 mg/kg of ST2518 (bright orange and dark orange labels respectively), ST1929 (pink and violet labels) or vehicle (white labels). A, optical imaging of one representative PPRE-*Luc* male mouse *per* group before (0 h) and

MOL #42689

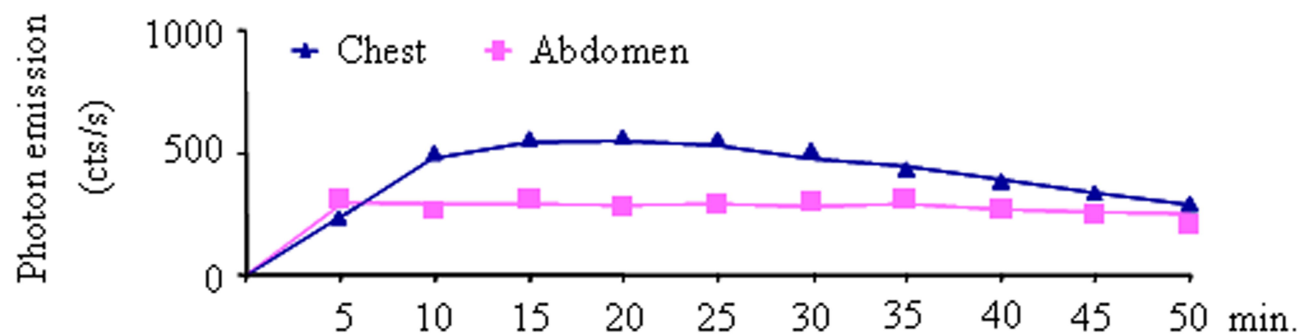
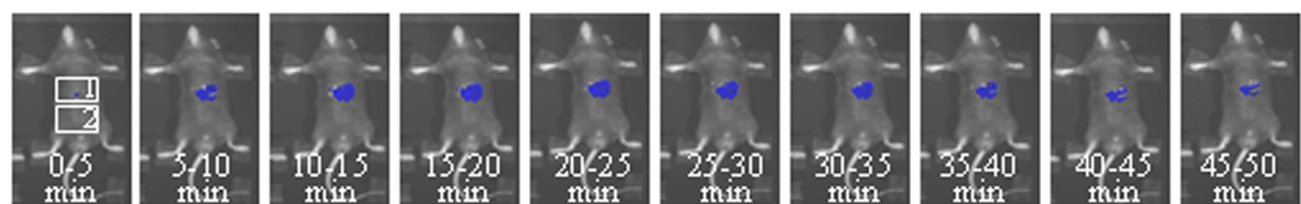
after 6 h treatment; B, photon emission expressed as counts for second (cts/s), detected by the imaging unit in chest, abdomen and testis before (0 h) and after 6 h treatment; C, luciferase activity (RLU) measured in protein extracts from liver, heart and testis after 6 h treatment. Bars represent the mean  $\pm$  S.E.M. of five mice. \*,  $P<0.05$  and \*\*,  $P<0.01$  as compared with vehicle treatment. P values were calculated with ANOVA followed by Bonferroni's test.

**Fig.7 - SPPARM activity of MK-886 in testis and lung revealed by the PPRE-*Luc* reporter mouse.**

PPRE-*Luc* mice were s.c. injected with: vehicle (white bars), 50 and 250 mg/kg Wy-14,643 (W50, grey bars and W250, black bars, respectively) and 250 mg/kg MK-886 administered alone (M250, diagonal striped bars) or 30 min before the 50 mg/kg Wy-14,643 treatment (W50+M250, vertical striped bars). Luciferase activity in testis was measured as photon emission (A) and as enzymatic activity in protein extracts from testis and lung (B). C, the expression of *Abcd2* and *Acox1*, two PPAR $\alpha$  target genes, was measured by semiquantitative real-time PCR assay on total mRNA extracted from testis and lung of mice treated for 6h with vehicle (white bars) and 250 mg/kg MK-886 (M250, diagonal striped bars). Bars represent the mean  $\pm$  SEM of at least five mice. \*,  $P<0.05$  versus 6h vehicle; °°,  $P<0.005$  versus 6h vehicle; °°°,  $P<0.001$  versus 6h vehicle. P values were calculated with ANOVA followed by Bonferroni's test (A and B) or by t-test (C). The experiment was repeated twice.

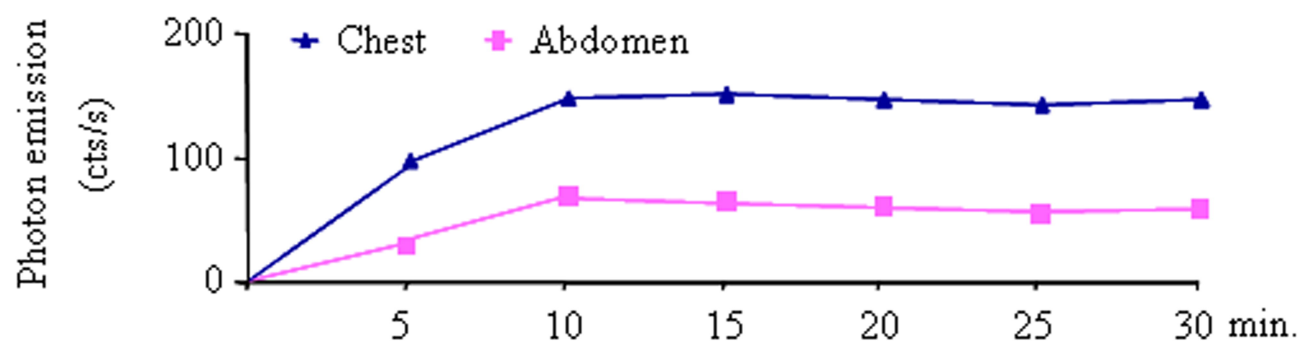
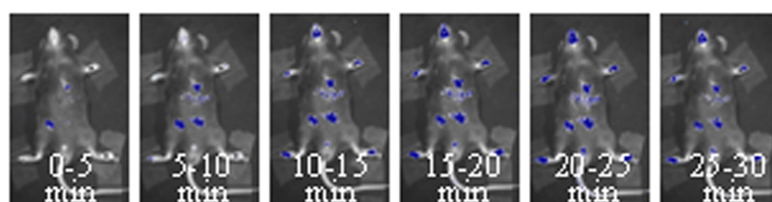
A

PPRE-Luc



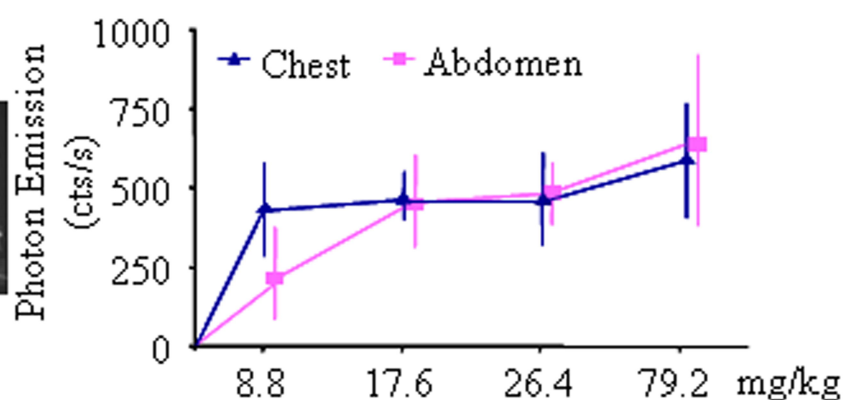
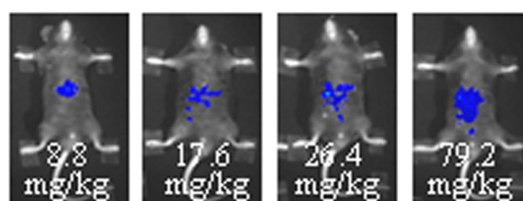
B

ERE-Luc



C

PPRE-Luc



D

ERE-Luc

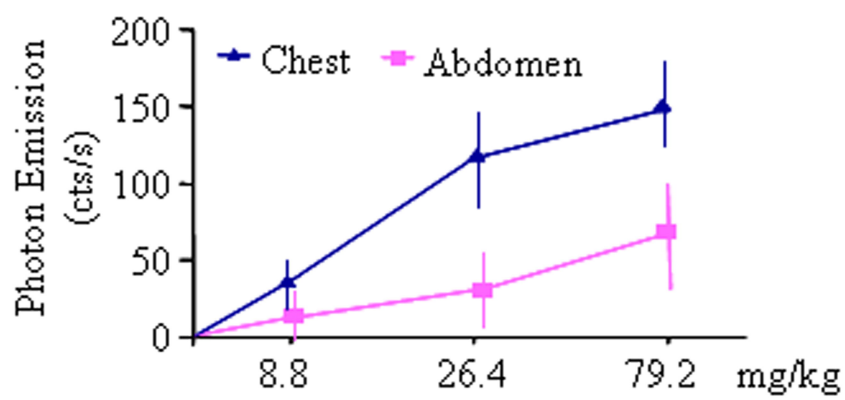
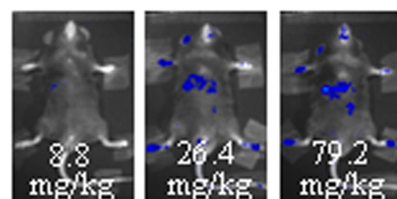


Figure 2

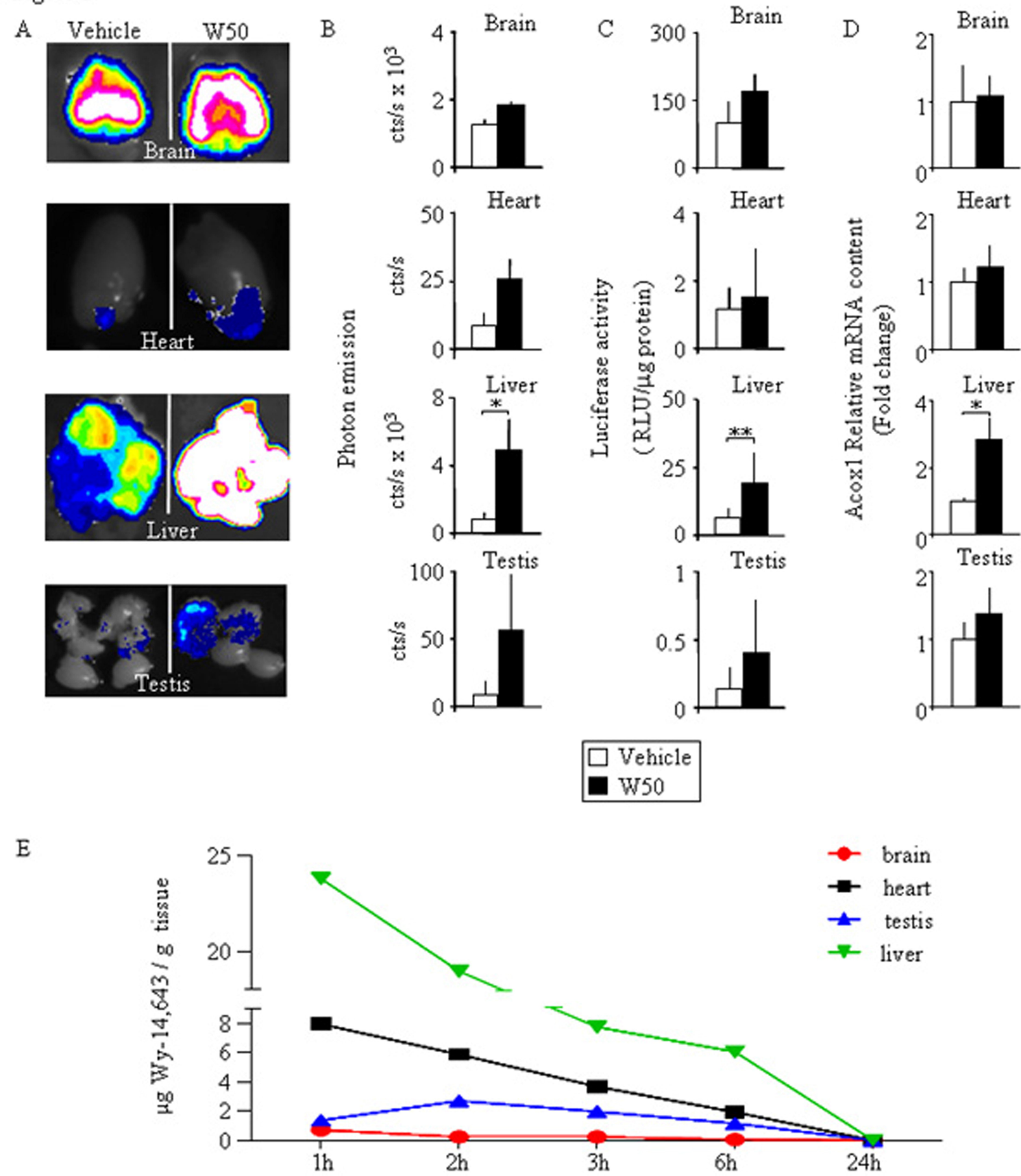




Figure 3

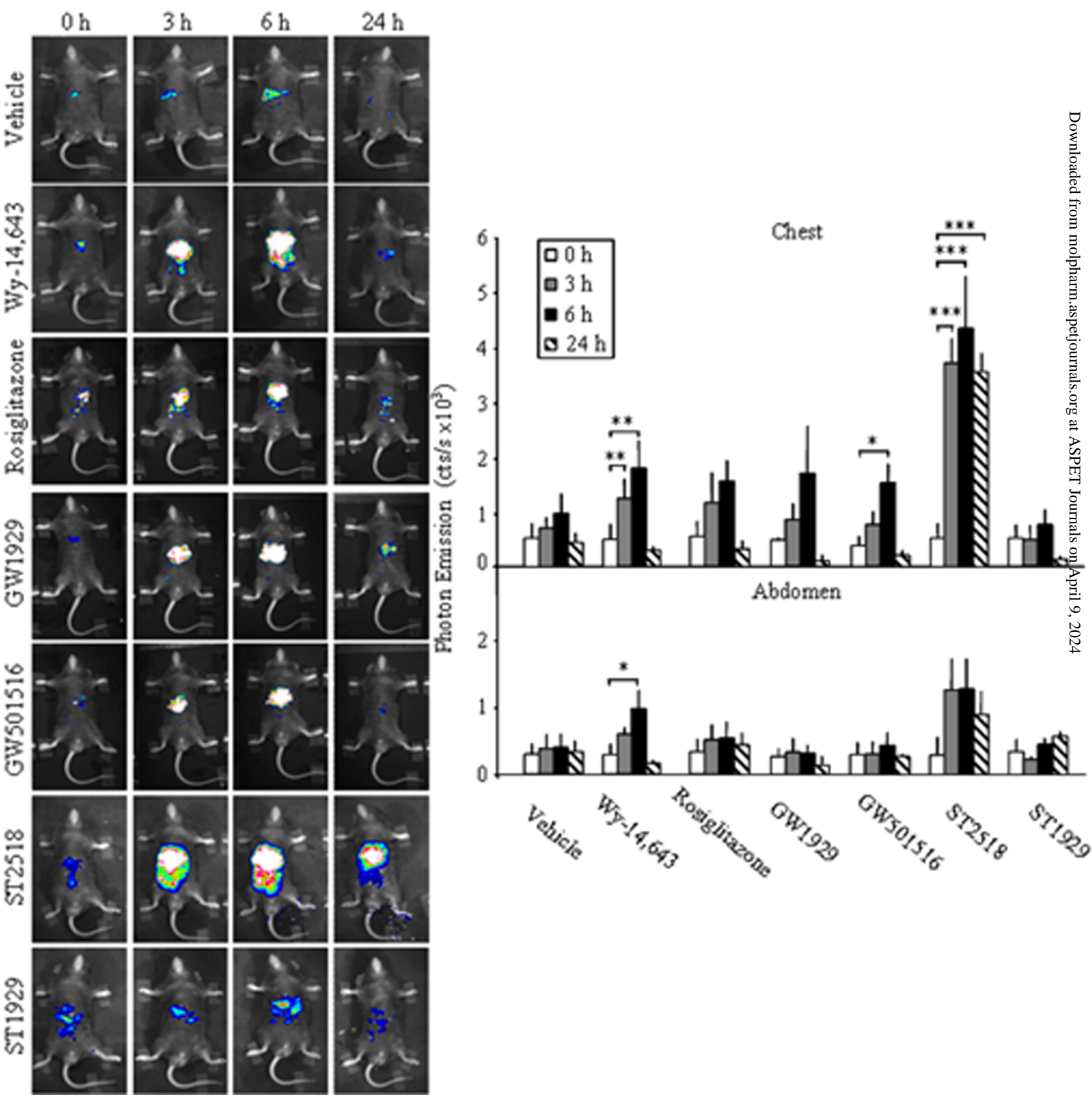


Figure 4

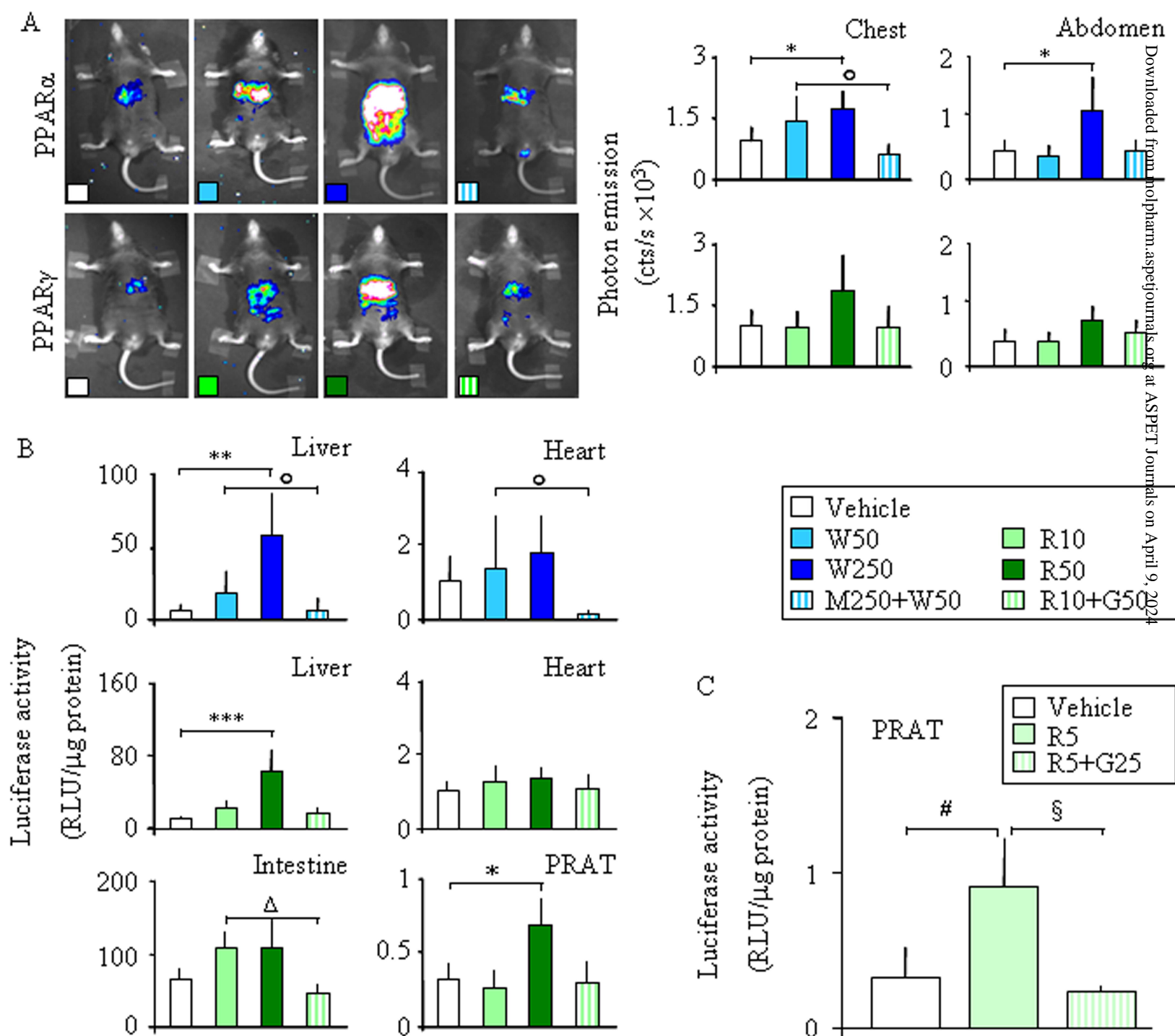


Figure 5

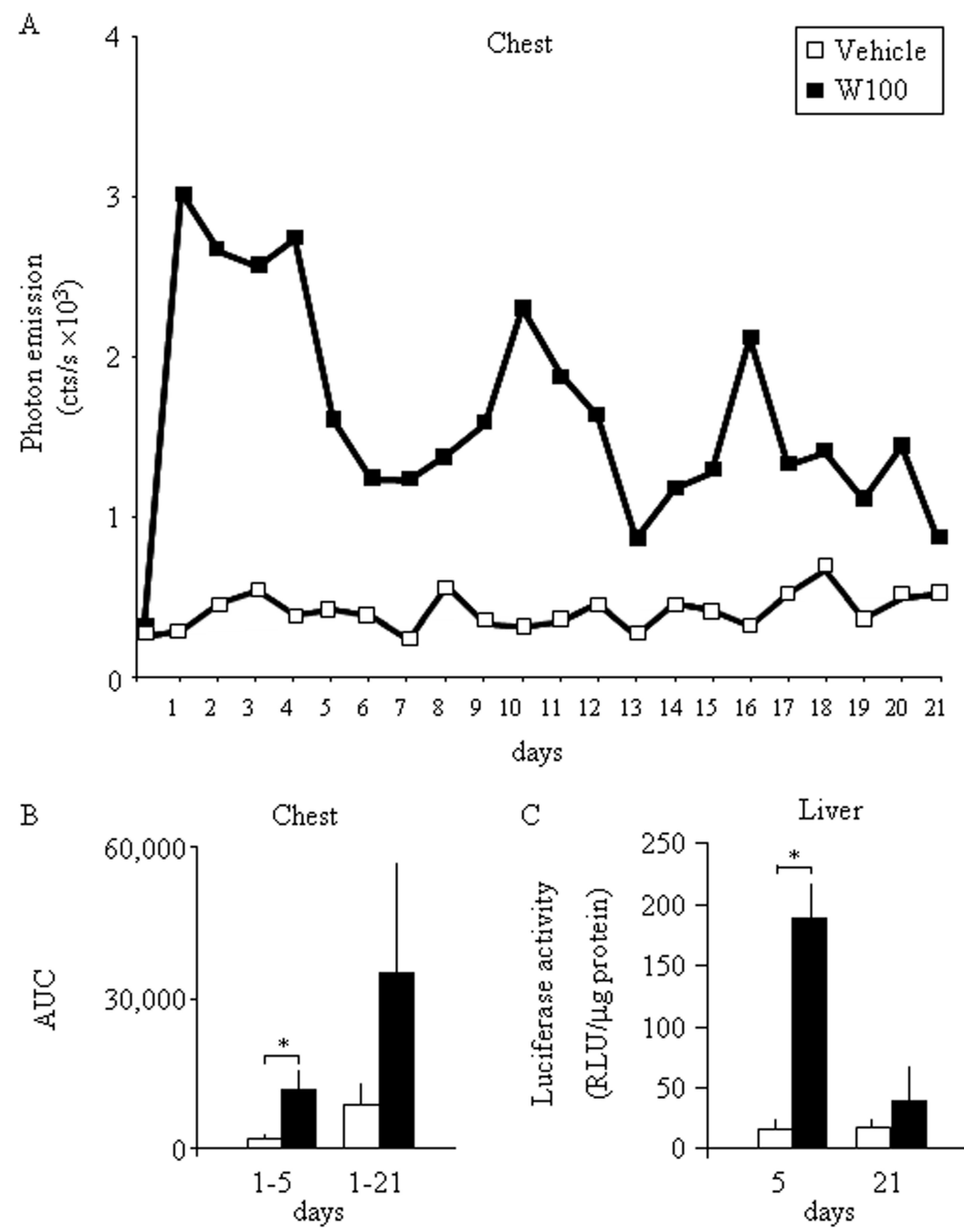


Figure 6

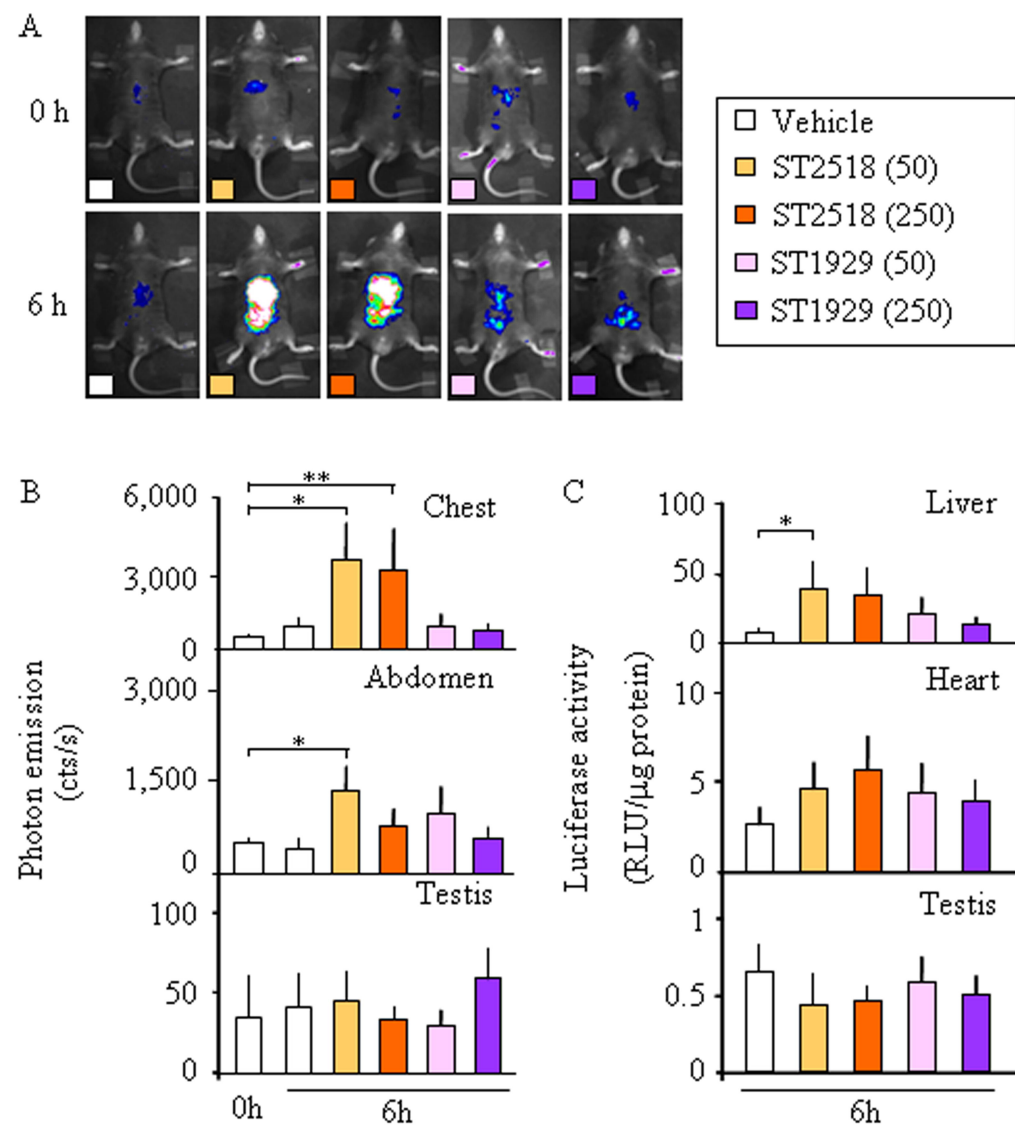


Figure 7

